Article
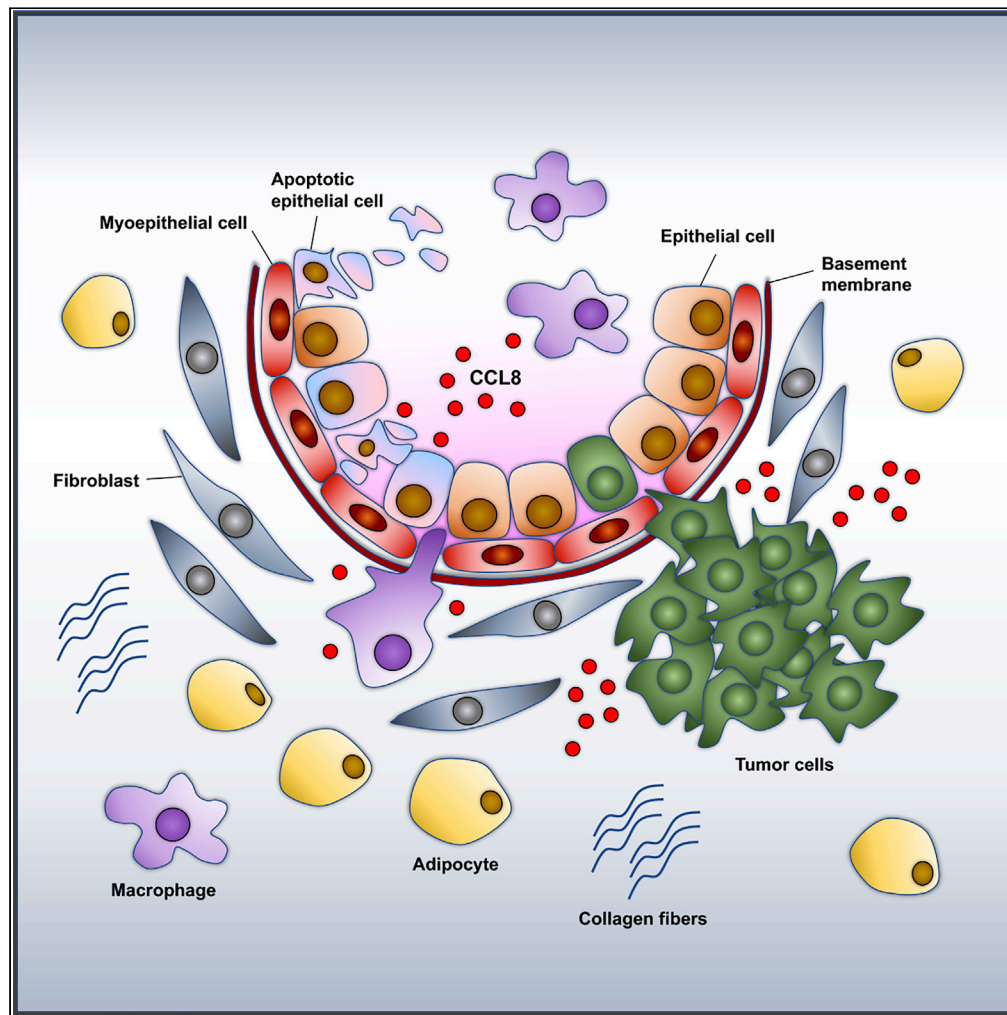
CCL8 Promotes Postpartum Breast Cancer by Recruiting M2 Macrophages

Elena Farmaki,
Vimala Kaza, Ioulia
Chatzistamou,
Hippokratis Kiaris

kiarish@cop.sc.edu

HIGHLIGHTS

CCL8 exhibits increased expression during mammary gland involution

CCL8 has tumor promoting activity and promotes postpartum breast cancer

Targeting CCL8 could have beneficial value for the management of postpartum breast cancer

Article

CCL8 Promotes Postpartum Breast Cancer by Recruiting M2 Macrophages

Elena Farmaki,[1] Vimala Kaza,[2] Ioulia Chatzistamou,[3] and Hippokratis Kiaris[1,2,4,*]

SUMMARY

The microenvironment of postpartum mammary gland promotes tumor growth and metastasis in animal models and is linked to increased risk of breast cancer and poor disease outcome in patients. Our previous studies showed the involvement of the chemokine CCL8 in breast cancer metastasis through modulation of the tumor-promoting activity of the tumor microenvironment. Here we show that CCL8 is highly expressed during mammary gland involution and enhances the infiltration of M2 subtype macrophages at the second phase of involution. Cancer cell inoculation studies in Ccl8-deficient animals indicate that CCL8 accelerates tumor onset during involution but not in nulliparous animals. Depletion of macrophages abolished the tumor-promoting effect of CCL8 in involution suggesting the specific role of CCL8 in promoting tumor growth by recruiting macrophages. These results underscore the role of CCL8 in the development of postpartum breast cancer and suggest the potential value of targeting CCL8 in disease management.

INTRODUCTION

Breast cancer is the most common cancer in women after skin cancer. Even though cancer mortality has been decreased, breast cancer remains a fatal disease, with 266,120 estimated new cases in the United States and an estimated mortality rate of 40,920 (https://seer.cancer.gov/statfacts/html/breast.html). The primary cause of death by breast cancer is the dissemination of the cancer cells prior to disease diagnosis and treatment that results in tumor growth at secondary sites and metastases (Fidler, 2003; Vanharanta and Massague, 2013).

Postpartum mammary cancer that includes breast cancers that develop within 10 years after child birth represents a distinct type of the disease that accounts for about 29% of all breast cancers for Caucasian women diagnosed ≤45 years (Goddard et al., 2019; Callihan et al., 2013). Postpartum breast cancer has a poor prognosis (Hartman and Eslick, 2016; Andersson et al., 2015; Johansson et al., 2011; Cottreau et al., 2019) compared with non-postpartum breast cancer or of that during pregnancy (Johansson et al., 2011; Van den Rul et al., 2011) because of increased risk of metastasis. Even though pregnancy has a protective effect against breast cancer, this effect is exerted only many years after childbirth (Ishida et al., 1992; Lambe et al., 1994). Contrarily, in a short period after pregnancy there is a transient risk for breast cancer that peaks between 5 and 10 years postpartum (Goddard et al., 2019; Schedin, 2006). Even though breast cancer death rates overall are decreasing, postpartum breast cancer remains a principal cause of mortality especially for young women (Goddard et al., 2019; Callihan et al., 2013).

Although the metastatic ability is inherent to the cancer cells, certain factors have been identified as potent activators of the process. One of these factors is mammary gland involution, a process in which the lactating gland returns to a morphologically nonsecretory pre-pregnant state and involves extensive tissue remodeling. Involution is characterized by the alveolar programmed cell death, mammary gland remodeling, and adipocyte repopulation (Strange et al., 1992; Zaragoza et al., 2015). The microenvironment of the involuting gland has been shown to be tumor promoting in different experimental mouse models (McDaniel et al., 2006; Martinson et al., 2015; Lyons et al., 2011; Bemis and Schedin, 2000). Involution occurs in two phases. The first one is reversible, is characterized by epithelial cell death, and is macrophage dependent (Lund et al., 1996; O'Brien et al., 2012). The second phase is non-reversible and is characterized by further cell death, accompanied by tissue-remodeling, collapsing of the lobuloalveolar structures, and adipocyte repopulation (Lund et al., 1996).

[1]Department of Drug Discovery and Biomedical Sciences, University of South Carolina, Columbia, SC 29208, USA

[2]Peromyscus Genetic Stock Center, University of South Carolina, Columbia, SC 29208, USA

[3]Department of Pathology, Microbiology and Immunology, University of South Carolina, School of Medicine, Columbia, SC 29209, USA

[4]Lead Contact

*Correspondence: kiarish@cop.sc.edu

https://doi.org/10.1016/j.isci.2020.101217

The mechanisms through which the microenvironment of involution promotes tumor growth include activated fibroblasts (Guo et al., 2017), increased fibrillar collagen, COX-2 (cyclooxygenase-2) overexpression from epithelial cells, abundant extracellular matrix (ECM) immune cell infiltration, and lymphangiogenesis (O'Brien et al., 2012; Li et al., 2017; Schedin et al., 2004; Lyons et al., 2014; Fornetti et al., 2014; Tamburini et al., 2019; Borges et al., 2016; Elder et al., 2018. Based on these findings therapeutic strategies have been proposed targeting either the immune cells such as immunotherapy (Fornetti et al., 2014) or non-steroidal anti-inflammatory drugs (NSAIDs) (Lyons et al., 2014; Pennock et al., 2018) for COX-2 inhibition and suppression of fibroblasts' tumor promoting activity (Guo et al., 2017).

The inflammatory microenvironment of involution is characterized by the upregulation of chemokines (Bambhroliya et al., 2018; Stein et al., 2009; Ron et al., 2007; Clarkson and Watson, 2003). Our previous studies showed the involvement of the chemokine CCL8 in cancer and metastasis through modulation of the tumor-promoting activity of the tumor microenvironment. *Ccl8* is a member of a conserved chemokine cluster, known as CC cluster, located in the conserved MCP region of the chromosome 11C in mice and 17q12 in humans (Nomiyama et al., 2001). CCL8 is involved in the immune response by attracting monocytes, T lymphocytes, natural killer cells (NK), basophils, mast cells, and eosinophils (Sozzani et al., 1994; Proost et al., 1996; Ruffing et al., 1998). According to our and others' results cancer cells can stimulate CCL8 production in adjacent stromal fibroblasts in breast and colon cancers (Farmaki et al., 2016, 2017; Torres et al., 2013). The prometastatic activity of CCL8 has been associated to the development of a CCL8 gradient between the neoplastic epithelium, the stroma, and the peripheral tissues and is correlated with poor prognosis in patients with breast cancer (Farmaki et al., 2016). This significance of CCL8 in regulating the directional movement of other cell types such as the innate lymphoid cells in the lungs was also recently confirmed and extended, underscoring the role of CCL8 in orchestrating cell migration in different pathophysiological conditions (Puttur et al., 2019).

In view of the extensive mobilization of various chemokines during mammary gland involution, in the present study we explored the specific role of CCL8 in the development of postpartum breast cancer.

RESULTS

CCL8 Expression Is Increased in the Mammary Gland during Involution

Publicly available microarray data show that Ccl8 is highly expressed during mammary gland involution, compared with the stages of puberty, pregnancy, and lactation (Ron et al., 2007) (Figure 1A). We confirmed this observation by qPCR analysis of Ccl8 mRNA levels in mammary glands from nulliparous mice or mice at involution day 4. The expression of Ccl8 mRNA in mice during involution was induced 4-fold ($p < 0.05$) compared with nulliparous mice (Figure 1B). In addition, mouse CCL8 protein levels measured by ELISA were 7-fold ($p < 0.05$) increased at involution day 5 and 4-fold increased at involution day 7 ($p < 0.05$) (Figure 1C).

To determine whether CCL8 loss affected mammary gland remodeling induced by involution, we performed histological analysis in mammary glands from wild-type (wt) or Ccl8KO mice. The deletion of CCL8 did not impair pregnancy or lactation. The histological appearance of the mammary glands from wt and Ccl8KO mice was similar during mammary involution, following the cessation of lactation (Figure S1A). The absence of morphological differences between wt and Ccl8KO mice was confirmed by quantification of the epithelial surface area occupying the glands (Figure S1B) and by assessment of β-casein protein levels by western blot (Figure S1C). These results indicate that CCL8 does not affect the remodeling of the mammary gland tissue during involution.

CCL8 Induces the Recruitment of Macrophages and Neutrophils in the Mammary Glands

Since CCL8 is involved in the inflammatory response (Proost et al., 1996), we investigated the infiltration of macrophages and neutrophils in the mammary glands from wt or Ccl8KO mice. Immunohistochemistry for the macrophage marker F4/80 and the neutrophil marker NM indicated that CCL8 is instrumental in recruiting macrophages during involution. As shown in Figure 2, following lactation a transient increase in the number of macrophages was detected in the mammary glands from wild-type mice during involution that peaked at day 5 ($p < 0.05$, $p < 0.001$) (Figures 2A and 2B). This effect was alleviated following *Ccl8* ablation suggesting that this chemokine is crucial for the recruitment of F4/80-positive macrophages, during involution. Similar trends, albeit insignificant, were also revealed for neutrophils implying a wider role for CCL8 in immune cell recruitment beyond macrophages (Figures 2C and 2D).
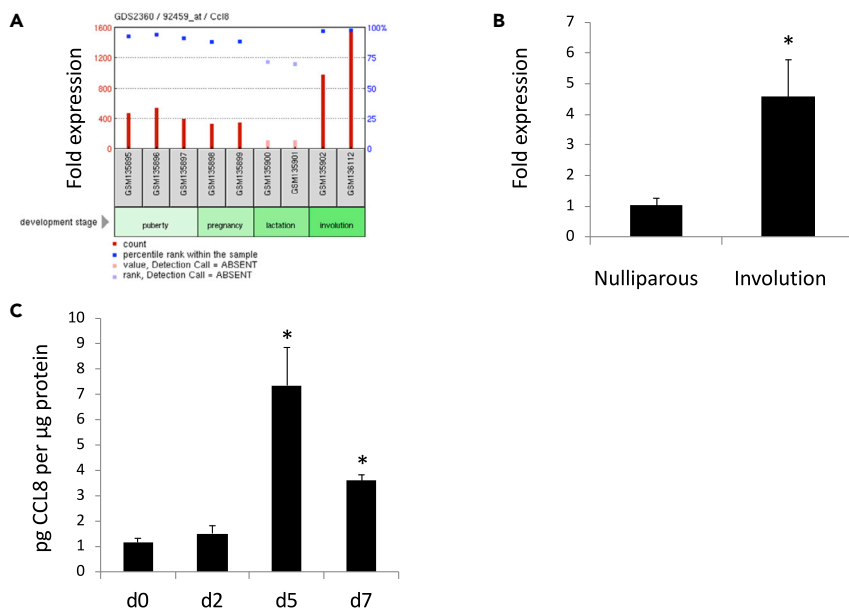
Figure 1. CCL8 Expression at Different Stages of Mammary Gland Development

(A) Microarray data using Affymetrix microarray (MG-U74v2) obtained from Ron et al. (2007) showing Ccl8 expression in mammary glands from C57B6 mice, puberty (6 weeks) (n = 3), pregnancy (14 days) (n = 2), lactation (10 days) (n = 2), and involution (4 days) (n = 2).

(B) Ccl8 gene expression in mammary glands from nulliparous mice or mice at involution day 4 (n = 4). Results are shown as average fold expression compared with nulliparous mice +SEM.

(C) CCL8 levels in mammary glands from wt mice at involution day 0 (lactation day 10) (n = 4), 2 (n = 2), 5 (n = 4), and 7 (n = 4). CCL8 levels were determined by ELISA. Results are shown as average +SEM (*, p < 0.05 Student's t test).

To dissect further the ability of CCL8 to attract tumor-promoting macrophages, we further determined the subtypes of M1 and M2 macrophages by staining for iNOS and arginase I, respectively, the mammary glands from wt and Ccl8KO mice at different days of involution. The results showed three times less M2 macrophages at involution day 7 in Ccl8KO mice compared with wt mice (Figures 2E and 2F), suggesting that CCL8 attracts primarily M2 macrophages, as opposed to the M1 macrophages, the number of which remained unaffected by the ablation of *Ccl8* (Figures 2G and 2H).

CCL8 Is Tumor Promoting during Involution

Based on the observation that CCL8 is a chemoattractant for M2 macrophages, which are known to be tumor promoting, we wanted to determine whether *Ccl8* ablation could directly affect the development of postpartum breast cancer at either the level of initiation or the level of progression. To explore this hypothesis, we introduced the *Ccl8*-null allele into an immunodeficient background (SCID) and mice, either nulliparous or during involution, were implanted with MCF10.DCIS.com breast cancer cells (Lyons et al., 2011). For comparison, MCF10.DCIS.com cells were implanted in SCID littermates that had the *Ccl8* gene intact. MCF10.DCIS.com cells were selected for this experiment because they had been used successfully in the past to study involution-associated breast cancer (Lyons et al., 2011). Consistently with earlier findings, tumorigenesis showed a positive trend during involution (Figure S2) (McDaniel et al., 2006; Martinson et al., 2015; Lyons et al., 2011; Bemis and Schedin, 2000). In the nulliparous females, no differences were observed between wt and Ccl8KO mice in both tumor growth rates and the period required for the development of palpable tumors (Figure 3A, pairwise comparisons in tumor growth of individual mice are shown). However, when cancer cells were injected at the second day of involution, after 10 days of lactation, the latency for tumor onset was drastically delayed in the *Ccl8*-deficient animals (p < 0.05) (Figure 3B). This finding suggests that CCL8 is tumor promoting only during involution but not in nulliparous animals. As soon as tumors were established their growth rate was not affected by CCL8, which in turn suggests that, although CCL8 is essential for tumor onset, it is not capable of affecting tumor progression, a notion that is also supported by the observation that histologically tumors in wt and Ccl8KO mice were indistinguishable (Figure 3D).
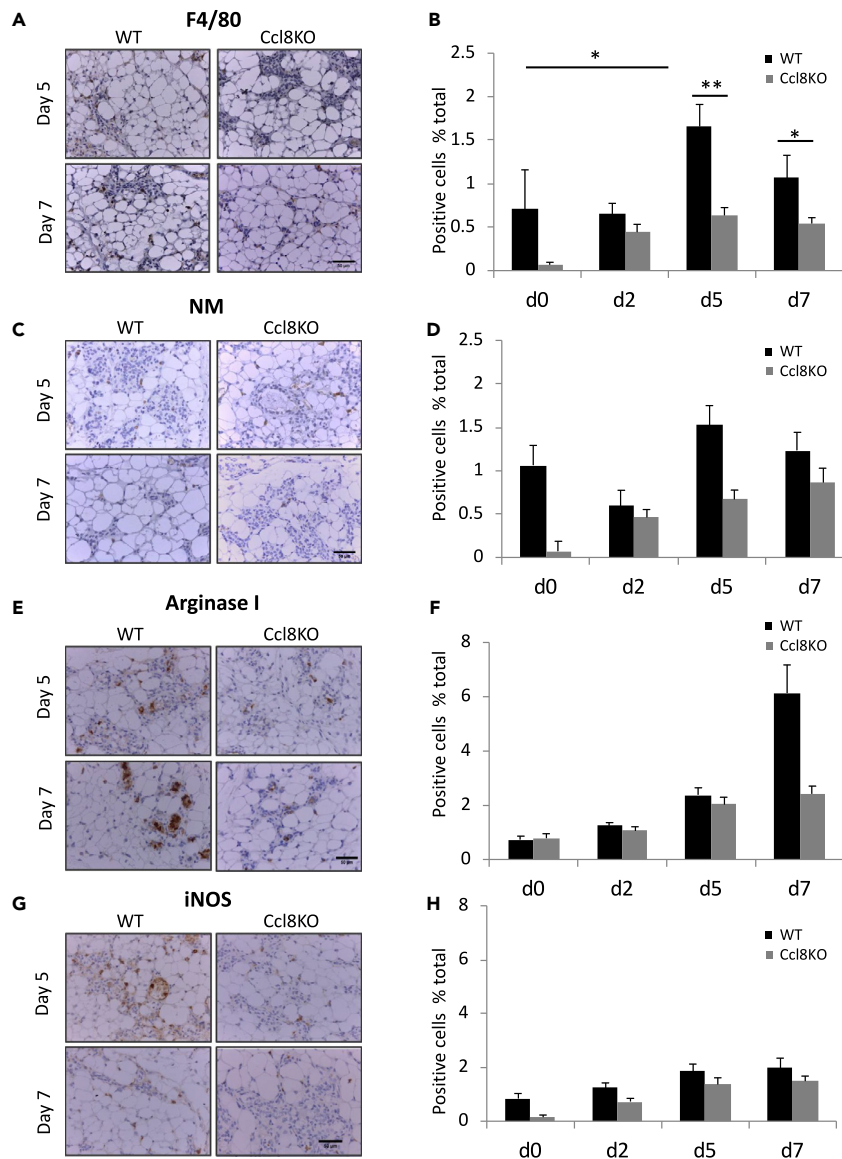
Figure 2. Macrophage and Neutrophil Recruitment in the Mammary Glands from Ccl8KO Mice at Different Stages of Mammary Gland Development

Representative images (40x) of mammary glands from wt or Ccl8KO mice at involution days 5 and 7 (n = 4) stained for F4/80 (A), neutrophil marker (NM) (C), Arginase I (E), and iNOS (G). Scale bar, 50 μm. Quantification of cells per optic field positive for F4/80 (B), NM (D), Arginase I (F), and iNOS (H) of the results described above. Results are shown as average + SEM (*, $p < 0.05$; **, $p < 0.001$ Student's t test).

The Tumor-Promoting Activity of CCL8 during Involution Involves M2 Macrophage Recruitment

The observation that CCL8 is tumor promoting, combined with the reduced infiltration of M2 macrophages in Ccl8KO mice during involution, predicts that ablation of macrophages would affect primarily wt and only minimally Ccl8KO animals. To test this hypothesis, we pharmacologically depleted macrophages by administration of clondronate liposomes (van Rooijen and Hendrikx, 2010) for 5 days, starting from lactation day 7 until involution day 2 and then injected cancer cells and monitored tumor onset and growth. The tumor-promoting effect of CCL8 during involution was abolished by macrophage depletion in the wt animals but did not affect Ccl8KO animals at which the tumor-promoting M2 macrophages were already diminished (Figure 3C). To rule out the possibility that clodronate influences tumorigenesis by impairing involution we administered clodronate
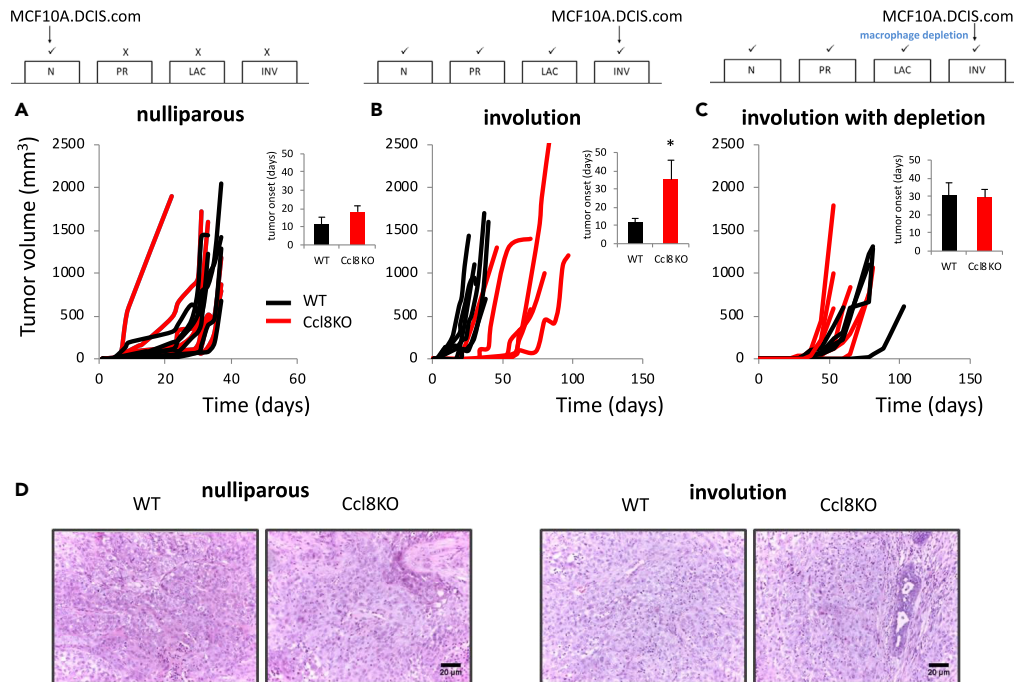
Figure 3. CCL8 Is Tumor Promoting during Involution

(A) Growth of MCF10.DCIS.com (2×10^5 cells) in SCID (wt) and Ccl8KOSCID (Ccl8KO) mice implanted in about 3-month nulliparous mice (n = 6). Results are shown as average +SEM.

(B) Growth of MCF10.DCIS.com (2×10^5 cells) in SCID (wt) and Ccl8KOSCID (Ccl8KO) mice implanted in day 2 of forced involution that followed 10 days of lactation (n = 6). The inset shows tumor onset in different groups. Results are shown as average + SEM (*, $p < 0.05$). See also Figure S2.

(C) Same as (B) with macrophage depletion (n = 5) starting from lactation day 7, using five daily intraperitoneal injections of 1 mg clodronate liposomes. See also Figures S3 and S4.

(D) Hematoxylin and eosin (H&E) in tumors from wt or Ccl8KO nulliparous mice or mice implanted in involution (n = 6). Scale bar, 20 μm in 20x. N, nulliparous; PR, pregnancy; LAC, lactation; INV, involution.

liposomes in wt and Ccl8KO mice and monitored the efficacy of post-lactation mammary gland remodeling; however, no differences between the wt and Ccl8KO mice were noted (Figures S4A and S4B).

To further determine whether CCL8 increases M2 subtype macrophage infiltration during tumorigenesis, we injected MCF10.DCIS.com cells enclosed in Matrigel in the mammary glands from wt or Ccl8KO SCID mice at involution day 2 and then recorded the number of M2 macrophages that are recruited by the newly implanted tumor in relation to the *Ccl8* status of the mammary glands. To that end, following 2 days of inoculation, cancer cell-containing Matrigel nodules implanted in wt and Ccl8KO mice were dissected and stained for the M2 marker arginase I. IHC indicated the decreased number of M2 subtype macrophages in the Matrigel nodules from Ccl8KO mice ($p < 0.05$) (Figures 4A and 4B). This finding is consistent with the specific ability of CCL8 to promote tumor growth by recruiting M2 macrophages (Figures 2E and 2F).

DISCUSSION

Postpartum breast cancer represents one of the most aggressive forms of breast cancer, but despite the progress, the options for specific therapeutic intervention against the disease are truly limited. In an attempt to explore specific therapeutic options for postpartum breast cancer management we investigated if modulation of CCL8 activity is linked to involution-associated promotion of tumor growth. Our results revealed an essential role for CCL8 in the promotion of involution-associated breast cancer that mechanistically was linked to the recruitment of the tumor-promoting M2 macrophages. Macrophages are recruited to the mammary gland at the second phase of involution (Martinson et al., 2015; O'Brien et al., 2010), and this effect, according to our present data, is mediated by CCL8 that is highly expressed during mammary gland involution. Noteworthy, the expression profile of CCL8 differed from that of CCL2 that is
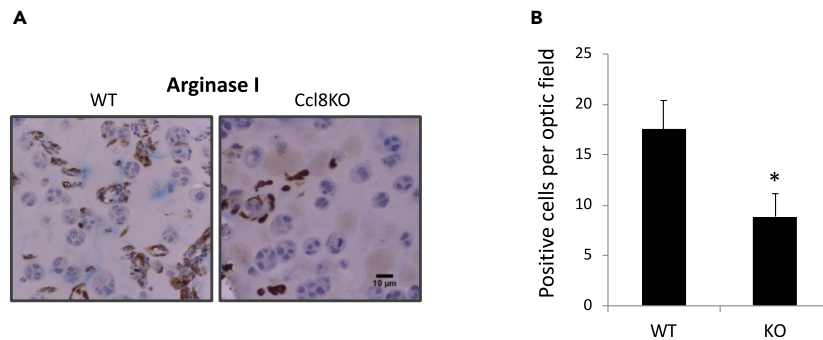
A

Arginase I

WT   Ccl8KO

B

Figure 4. CCL8 Promotes Tumor Growth by Recruiting M2 Macrophages

(A) Representative images (20x) of mammary glands stained for Arginase I from SCID (wt) and Ccl8KOSCID (Ccl8KO) mice implanted with MCF10.DCIS.com (1x10^6 cells) enclosed in Matrigel at day 2 of forced involution that followed 10 days of lactation (n = 5). Animals were sacrificed 2 days later. Scale bar, 10 μm.

(B) Quantification of cells per optic field positive for Arginase I of the results described above. Results are shown as average + SEM (*, $p < 0.05$, Student's t test).

structurally related to CCL8 and encoded by a gene located in the same chemokine cluster with CCL8 (Nomiyama et al., 2001). CCL2 protein levels had a peak at day 2 of involution followed by a decrease (O'Brien et al., 2010; Mantovani et al., 2004), contrary to the protein levels of CCL8 that peaked at day 5 and maintained high until day 7. These findings imply that CCL8 might have different functions and apparently different regulation during involution compared with other chemokines that are members of the same cluster (Nomiyama et al., 2001). This is also suggested by the fact that despite *Ccl8* ablation reduced macrophage numbers in the mammary gland during involution, tissue remodeling was not delayed during involution. Direct activities of CCL8 onto the mammary epithelial cells, in combination with its delayed expression profile as compared with other chemoattractive cytokines of the same cluster, may offset the anticipated delay in involution due to macrophage depletion.

Furthermore, CCL8 causes increased infiltration of M2 subtype macrophages specifically at involution day 7. Consistent with this result is the high expression of the receptors CCR1 and CCR5 in M2 macrophages compared with M1 (Xuan et al., 2015) that are receptors for CCL8 (Proost et al., 1996; Sozzani et al., 1995; Ruffing et al., 1998).

In the context of involution-associated tumorigenesis, ablation of *Ccl8* significantly delayed the onset of breast tumors during involution, whereas in nulliparous mice it had no effect. This finding suggests that in the absence of CCL8 tumor growth is considerably impeded, rendering CCL8 as a major determinant of the tumor-promoting activity of involution. The fact that histology or tumor growth rates did not differ in tumors from wt and Ccl8KO mice indicates that CCL8 affects tumor initiation by developing a proinflammatory microenvironment but not the morphogenesis of tumors or their development beyond onset. To further support this notion, *in vivo* depletion of macrophages abolished the tumor-promoting effect of CCL8 during involution, only in wt animals. A limitation of this strategy for macrophage depletion is that clodronate was shown capable of depleting additional immune cells in peripheral tissues such as dendritic cells (Ward et al., 2012; Konig et al., 2014; Kitamoto et al., 2009; Lu et al., 2012), which may also contribute directly or indirectly to the remodeling of the mammary gland during involution. Nevertheless, despite this limitation, in animals with disrupted macrophage function, tumor onset was similar in the wt and the *Ccl8*-deficient groups suggesting that the tumor-promoting action of CCL8 in involution is strictly dependent on the presence of macrophages. Consistently with this notion, CCL8 was recently identified as a part of the breast tumor associated macrophages (TAM) signature in humans (Cassetta et al., 2019). Macrophages play a crucial role in the normal postpartum mammary gland involution (O'Brien et al., 2012), and specifically the M2 subtype of macrophages promotes the development of a proinflammatory and protumorigenic microenvironment during involution (O'Brien et al., 2010). In our experimental model, CCL8 facilitates the infiltration of M2 macrophages in the presence of cancer cells during involution and accelerates tumor onset.

Our previously published results (Farmaki et al., 2016) show that stromal cells and especially fibroblasts constitute a primary source of CCL8 and that breast cancer cells activate CCL8 expression in fibroblasts.

Consistent with these results, recent studies show that activated mammary fibroblasts within the involuting mammary gland have protumorigenic function that can be suppressed by NSAIDs (Guo et al., 2017).

Collectively our data show that CCL8 is instrumental for the pathogenesis of postpartum breast cancers by attracting tumor-promoting macrophages during involution. These results, combined also with the finding that inhibition of CCL8 does not affect physiological mammary function, suggest the potential value of CCL8 as a target molecule for the management of postpartum breast cancers.

Limitations of the Study

In the present study, we used a mouse model of immunodeficient transgenic animals for the tumor growth studies. The findings need to be replicated in a syngeneic model to include the immune responses of the hosts. For *in vivo* macrophage depletion we used clodronate liposomes. However, clodronate was found to deplete additional immune cells such as dendritic cells in the skin and kidney. Evaluation of the effect of clodronate on immune cells other than macrophages in the mammary gland and the physiological implications may be considered.

Resource Availability

Lead Contact

Correspondence and requests for materials and reagents should be addressed to the Lead Contact, Hippokratis Kiaris (kiarish@cop.sc.edu).

Materials Availability

This study did not generate new unique reagents. The Ccl8KO mice in this study are available from the Lead Contact.

Data and Code Availability

This study did not generate any new data or code.

METHODS

All methods can be found in the accompanying Transparent Methods supplemental file.

SUPPLEMENTAL INFORMATION

Supplemental Information can be found online at https://doi.org/10.1016/j.isci.2020.101217.

AUTHOR CONTRIBUTIONS

E.F. designed and performed experiments, interpreted results, and drafted the manuscript. V.K. performed experiments and interpreted results. I.C. performed histopathology, interpreted results, and edited the manuscript. H.K. designed experiments, interpreted results, and drafted the manuscript. All authors read and approved the final manuscript.

DECLARATION OF INTERESTS

The University of South Carolina has applied for a patent for neutralizing monoclonal antibodies against hCCL8 (US20190359700A1). The authors are designated as inventors in this patent application.

REFERENCES

Andersson, T.M., Johansson, A.L., Fredriksson, I., and Lambe, M. (2015). Cancer during pregnancy and the postpartum period: a population-based study. Cancer 121, 2072–2077.

Bambhroliya, A., Van Wyhe, R.D., Kumar, S., Debeb, B.G., Reddy, J.P., Van Laere, S., El-Zein, R., Rao, A., and Woodward, W.A. (2018). Gene set analysis of post-lactational mammary gland involution gene signatures in inflammatory and triple-negative breast cancer. PLoS One 13, e0192689.

Bemis, L.T., and Schedin, P. (2000). Reproductive state of rat mammary gland stroma modulates human breast cancer cell migration and invasion. Cancer Res. 60, 3414–3418.

Borges, V.F., Elder, A.M., and Lyons, T.R. (2016). Deciphering pro-lymphangiogenic programs during mammary involution and postpartum breast cancer. Front. Oncol. 6, 227.

Callihan, E.B., Gao, D., Jindal, S., Lyons, T.R., Manthey, E., Edgerton, S., Urquhart, A., Schedin, P., and Borges, V.F. (2013). Postpartum diagnosis demonstrates a high risk for metastasis and merits an expanded definition of pregnancy-associated breast cancer. Breast Cancer Res. Treat. 138, 549–559.

Cassetta, L., Fragkogianni, S., Sims, A.H., Swierczak, A., Forrester, L.M., Zhang, H., Soong, D.Y.H., Cotechini, T., Anur, P., Lin, E.Y., et al. (2019). Human tumor-associated macrophage and monocyte transcriptional landscapes reveal cancer-specific reprogramming, biomarkers, and therapeutic targets. Cancer Cell 35, 588–602.e10.

Clarkson, R.W., and Watson, C.J. (2003). Microarray analysis of the involution switch. J. Mammary Gland Biol. Neoplasia 8, 309–319.

Cottreau, C.M., Dashevsky, I., Andrade, S.E., Li, D.K., Nekhlyudov, L., Raebel, M.A., Ritzwoller, D.P., Partridge, A.H., Pawloski, P.A., and Toh, S. (2019). Pregnancy-associated cancer: a U.S. population-based study. J. Womens Health (Larchmt) 28, 250–257.

Elder, A.M., Tamburini, B.A., Crump, L.S., Black, S.A., Wessells, V.M., Schedin, P.J., Borges, V.F., and Lyons, T.R. (2018). Semaphorin 7A promotes macrophage-mediated lymphatic remodeling during postpartum mammary gland involution and in breast cancer. Cancer Res. 78, 6473–6485.

Farmaki, E., Kaza, V., Papavassiliou, A.G., Chatzistamou, I., and Kiaris, H. (2017). Induction of the MCP chemokine cluster cascade in the periphery by cancer cell-derived Ccl3. Cancer Lett. 389, 49–58.

Farmaki, E., Chatzistamou, I., Kaza, V., and Kiaris, H. (2016). A CCL8 gradient drives breast cancer cell dissemination. Oncogene 35, 6309–6318.

Fidler, I.J. (2003). The pathogenesis of cancer metastasis: the 'seed and soil' hypothesis revisited. Nat. Rev. Cancer 3, 453–458.

Fornetti, J., Martinson, H.A., Betts, C.B., Lyons, T.R., Jindal, S., Guo, Q., Coussens, L.M., Borges, V.F., and Schedin, P. (2014). Mammary gland involution as an immunotherapeutic target for postpartum breast cancer. J. Mammary Gland Biol. Neoplasia 19, 213–228.

Goddard, E.T., Bassale, S., Schedin, T., Jindal, S., Johnston, J., Cabral, E., Latour, E., Lyons, T.R., Mori, M., Schedin, P.J., et al. (2019). Association between postpartum breast cancer diagnosis and metastasis and the clinical features underlying risk. JAMA Netw. Open 2, e186997.

Guo, Q., Minnier, J., Burchard, J., Chiotti, K., Spellman, P., and Schedin, P. (2017). Physiologically activated mammary fibroblasts promote postpartum mammary cancer. JCI Insight 2, e89206.

Hartman, E.K., and Eslick, G.D. (2016). The prognosis of women diagnosed with breast cancer before, during and after pregnancy: a meta-analysis. Breast Cancer Res. Treat. 160, 347–360.

Ishida, T., Yokoe, T., Kasumi, F., Sakamoto, G., Makita, M., Tominaga, T., Simozuma, K., Enomoto, K., Fujiwara, K., Nanasawa, T., et al. (1992). Clinicopathologic characteristics and prognosis of breast cancer patients associated with pregnancy and lactation: analysis of case-control study in Japan. Jpn. J. Cancer Res. 83, 1143–1149.

Johansson, A.L., Andersson, T.M., Hsieh, C.C., Cnattingius, S., and Lambe, M. (2011). Increased mortality in women with breast cancer detected during pregnancy and different periods postpartum. Cancer Epidemiol. Biomarkers Prev. 20, 1865–1872.

Kitamoto, K., Machida, Y., Uchida, J., Izumi, Y., Shiota, M., Nakao, T., Iwao, H., Yukimura, T., Nakatani, T., and Miura, K. (2009). Effects of liposome clodronate on renal leukocyte populations and renal fibrosis in murine obstructive nephropathy. J. Pharmacol. Sci. 111, 285–292.

Konig, S., Nitzki, F., Uhmann, A., Dittmann, K., Theiss-Suennemann, J., Herrmann, M., Reichardt, H.M., Schwendener, R., Pukrop, T., Schulz-Schaeffer, W., et al. (2014). Depletion of cutaneous macrophages and dendritic cells promotes growth of basal cell carcinoma in mice. PLoS One 9, e93555.

Lambe, M., Hsieh, C., Trichopoulos, D., Ekbom, A., Pavia, M., and Adami, H.O. (1994). Transient increase in the risk of breast cancer after giving birth. N. Engl. J. Med. 331, 5–9.

Li, Y., Pang, Z., Dong, X., Liao, X., Deng, H., Liao, C., Liao, Y., Chen, G., and Huang, L. (2017). MUC1 induces M2 type macrophage influx during postpartum mammary gland involution and triggers breast cancer. Oncotarget 9, 3446–3458.

Lu, L., Faubel, S., He, Z., Andres Hernando, A., Jani, A., Kedl, R., and Edelstein, C.L. (2012). Depletion of macrophages and dendritic cells in ischemic acute kidney injury. Am. J. Nephrol. 35, 181–190.

Lund, L.R., Romer, J., Thomasset, N., Solberg, H., Pyke, C., Bissell, M.J., Dano, K., and Werb, Z. (1996). Two distinct phases of apoptosis in mammary gland involution: proteinase-independent and -dependent pathways. Development 122, 181–193.

Lyons, T.R., Borges, V.F., Betts, C.B., Guo, Q., Kapoor, P., Martinson, H.A., Jindal, S., and Schedin, P. (2014). Cyclooxygenase-2-dependent lymphangiogenesis promotes nodal metastasis of postpartum breast cancer. J. Clin. Invest. 124, 3901–3912.

Lyons, T.R., O'Brien, J., Borges, V.F., Conklin, M.W., Keely, P.J., Eliceiri, K.W., Marusyk, A., Tan, A.C., and Schedin, P. (2011). Postpartum mammary gland involution drives progression of ductal carcinoma in situ through collagen and COX-2. Nat. Med. 17, 1109–1115.

Mantovani, A., Sica, A., Sozzani, S., Allavena, P., Vecchi, A., and Locati, M. (2004). The chemokine system in diverse forms of macrophage activation and polarization. Trends Immunol. 25, 677–686.

Martinson, H.A., Jindal, S., Durand-Rougely, C., Borges, V.F., and Schedin, P. (2015). Wound healing-like immune program facilitates postpartum mammary gland involution and tumor progression. Int. J. Cancer 136, 1803–1813.

McDaniel, S.M., Rumer, K.K., Biroc, S.L., Metz, R.P., Singh, M., Porter, W., and Schedin, P. (2006). Remodeling of the mammary microenvironment after lactation promotes breast tumor cell metastasis. Am. J. Pathol. 168, 608–620.

Nomiyama, H., Mera, A., Ohneda, O., Miura, R., Suda, T., and Yoshie, O. (2001). Organization of the chemokine genes in the human and mouse major clusters of CC and CXC chemokines: diversification between the two species. Genes Immun. 2, 110–113.

O'Brien, J., Lyons, T., Monks, J., Lucia, M.S., Wilson, R.S., Hines, L., Man, Y.G., Borges, V., and Schedin, P. (2010). Alternatively activated macrophages and collagen remodeling characterize the postpartum involuting mammary gland across species. Am. J. Pathol. 176, 1241–1255.

O'Brien, J., Martinson, H., Durand-Rougely, C., and Schedin, P. (2012). Macrophages are crucial for epithelial cell death and adipocyte repopulation during mammary gland involution. Development 139, 269–275.

Pennock, N.D., Martinson, H.A., Guo, Q., Betts, C.B., Jindal, S., Tsujikawa, T., Coussens, L.M., Borges, V.F., and Schedin, P. (2018). Ibuprofen supports macrophage differentiation, T cell recruitment, and tumor suppression in a model of postpartum breast cancer. J. Immunother. Cancer 6, 98.

Proost, P., Wuyts, A., and Van Damme, J. (1996). Human monocyte chemotactic proteins-2 and -3: structural and functional comparison with MCP-1. J. Leukoc. Biol. 59, 67–74.

Puttur, F., Denney, L., Gregory, L.G., Vuononvirta, J., Oliver, R., Entwistle, L.J., Walker, S.A., Headley, M.B., McGhee, E.J., Pease, J.E., et al. (2019). Pulmonary environmental cues drive group 2 innate lymphoid cell dynamics in mice and humans. Sci. Immunol. 4, eaav7638.

Ron, M., Israeli, G., Seroussi, E., Weller, J.I., Gregg, J.P., Shani, M., and Medrano, J.F. (2007). Combining mouse mammary gland gene expression and comparative mapping for the

identification of candidate genes for QTL of milk production traits in cattle. BMC Genomics *8*, 183.

Ruffing, N., Sullivan, N., Sharmeen, L., Sodroski, J., and Wu, L. (1998). CCR5 has an expanded ligand-binding repertoire and is the primary receptor used by MCP-2 on activated T cells. Cell Immunol. *189*, 160–168.

Schedin, P. (2006). Pregnancy-associated breast cancer and metastasis. Nat. Rev. Cancer *6*, 281–291.

Schedin, P., Mitrenga, T., McDaniel, S., and Kaeck, M. (2004). Mammary ECM composition and function are altered by reproductive state. Mol. Carcinog. *41*, 207–220.

Sozzani, S., Locati, M., Zhou, D., Rieppi, M., Luini, W., Lamorte, G., Bianchi, G., Polentarutti, N., Allavena, P., and Mantovani, A. (1995). Receptors, signal transduction, and spectrum of action of monocyte chemotactic protein-1 and related chemokines. J. Leukoc. Biol. *57*, 788–794.

Sozzani, S., Zhou, D., Locati, M., Rieppi, M., Proost, P., Magazin, M., Vita, N., van Damme, J., and Mantovani, A. (1994). Receptors and transduction pathways for monocyte chemotactic protein-2 and monocyte chemotactic protein-3.

Similarities and differences with MCP-1. J. Immunol. *152*, 3615–3622.

Stein, T., Salomonis, N., Nuyten, D.S., van de Vijver, M.J., and Gusterson, B.A. (2009). A mouse mammary gland involution mRNA signature identifies biological pathways potentially associated with breast cancer metastasis. J. Mammary Gland Biol. Neoplasia *14*, 99–116.

Strange, R., Li, F., Saurer, S., Burkhardt, A., and Friis, R.R. (1992). Apoptotic cell death and tissue remodelling during mouse mammary gland involution. Development *115*, 49–58.

Tamburini, B.A.J., Elder, A.M., Finlon, J.M., Winter, A.B., Wessells, V.M., Borges, V.F., and Lyons, T.R. (2019). PD-1 blockade during post-partum involution reactivates the anti-tumor response and reduces lymphatic vessel density. Front. Immunol. *10*, 1313.

Torres, S., Bartolome, R.A., Mendes, M., Barderas, R., Fernandez-Acenero, M.J., Pelaez-Garcia, A., Pena, C., Lopez-Lucendo, M., and Villar-Vazquez, R. (2013). Proteome profiling of cancer-associated fibroblasts identifies novel proinflammatory signatures and prognostic markers for colorectal cancer. Clin. Cancer Res. *19*, 6006–6019.

Van den Rul, N., Han, S.N., Van Calsteren, K., Neven, P., and Amant, F. (2011). Postpartum breast cancer behaves differently. Facts Views Vis. Obgyn. *3*, 183–188.

van Rooijen, N., and Hendrikx, E. (2010). Liposomes for specific depletion of macrophages from organs and tissues. Methods Mol. Biol. *605*, 189–203.

Vanharanta, S., and Massague, J. (2013). Origins of metastatic traits. Cancer Cell *24*, 410–421.

Ward, N.L., Loyd, C.M., Wolfram, J.A., Diaconu, D., Michaels, C.M., and McCormick, T.S. (2012). Depletion of antigen-presenting cells by clodronate liposomes reverses the psoriatic skin phenotype in KC-Tie2 mice. Br. J. Dermatol. *164*, 750–758.

Xuan, W., Qu, Q., Zheng, B., Xiong, S., and Fan, G.H. (2015). The chemotaxis of M1 and M2 macrophages is regulated by different chemokines. J. Leukoc. Biol. *97*, 61–69.

Zaragoza, R., Garcia-Trevijano, E.R., Lluch, A., Ribas, G., and Vina, J.R. (2015). Involvement of Different networks in mammary gland involution after the pregnancy/lactation cycle: implications in breast cancer. IUBMB Life *67*, 227–238.

Supplemental Information

CCL8 Promotes Postpartum Breast Cancer

by Recruiting M2 Macrophages

Elena Farmaki, Vimala Kaza, Ioulia Chatzistamou, and Hippokratis Kiaris
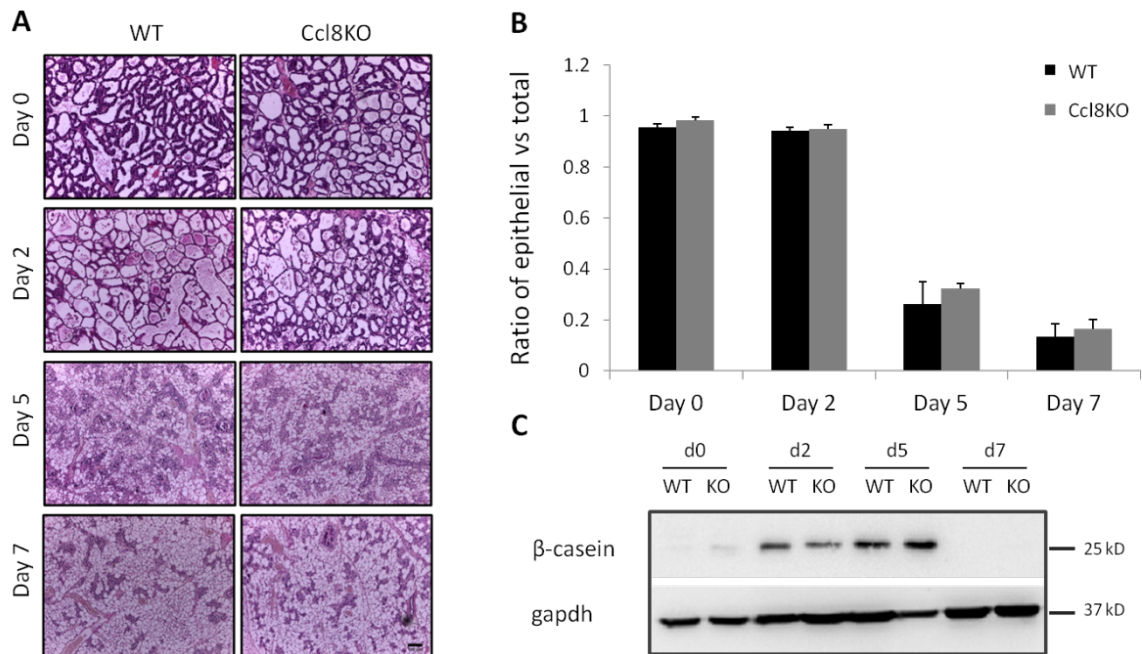
Supplemental Figures

Figure S1. Histological analysis of mammary glands from wt and Ccl8KO mice at different stages of mammary gland development. Related to Figure 1. (A) Hematoxylin and eosin (H&E) staining in the mammary glands from wt or Ccl8KO mice at involution day 0 (lactation day 10), 2, 5 and 7 (n=3). Scale bar 100μm in 10x. (B) Quantification of the epithelial surface by image analysis. Results are shown as average + SD. (C) Representative image of β-casein levels in mammary glands from wt or Ccl8KO mice at involution day 0 (lactation day 10), 2, 5 and 7 assessed by immunoblot.
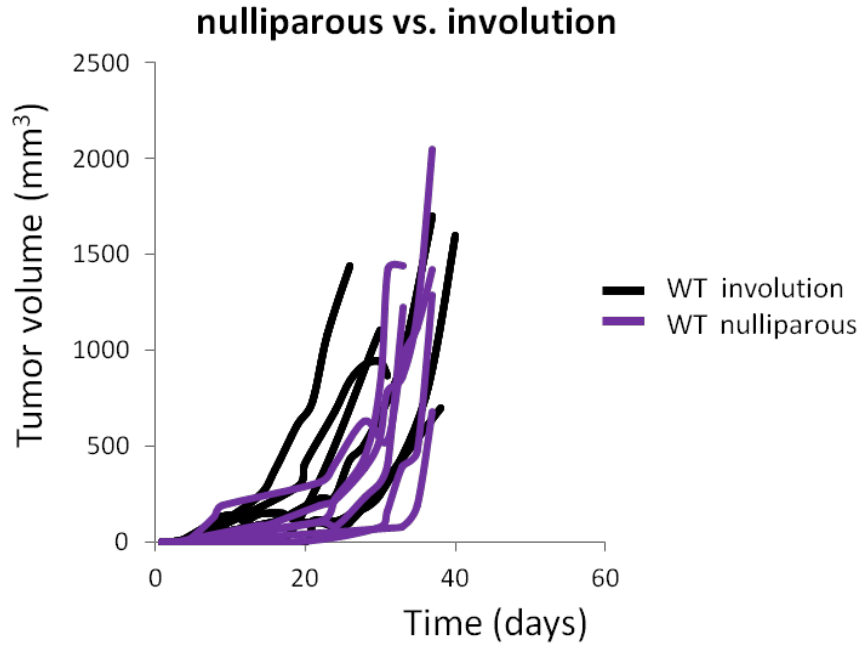
Figure S2. Tumor growth in nulliparous SCID mice and SCID mice during involution, Related to Figures 3A and 3B. MCF10.DCIS.com ($2x10^5$ cells) were implanted in about 3 month SCID nulliparous mice (n=6, purple lines) or in SCID mice at day 2 of forced involution that followed 10 days of lactation (n=6, black lines).
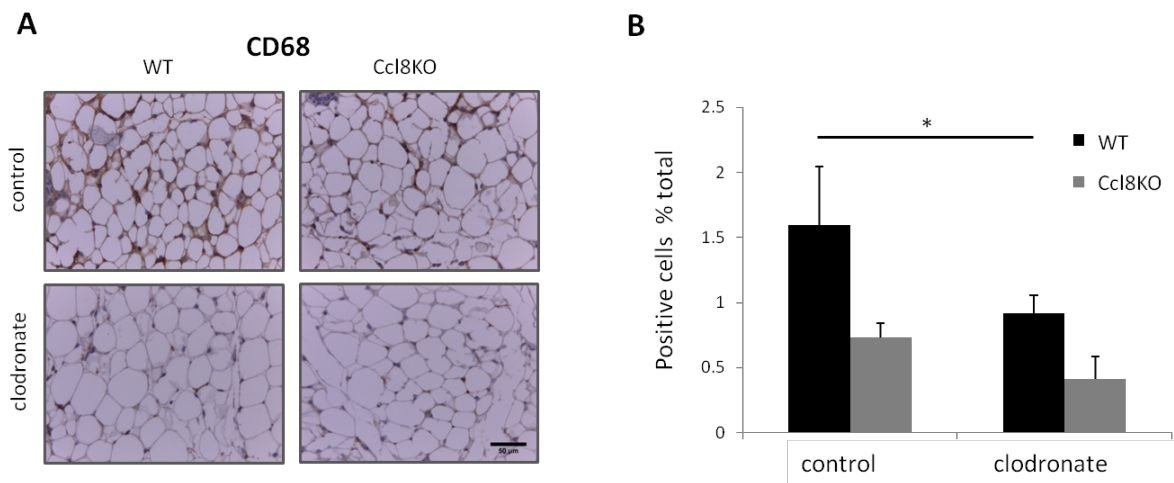

Figure S3. Macrophage depletion in the mammary glands from wt and Ccl8KO, Related to Figure 3C. (A) Representative images (40x) of mammary glands from wt or Ccl8KO CB7B6 mice stained for the macrophage marker CD68 after 5 daily ip injections of 1mg clodronate liposomes. Scale bar 50μm. (B) Quantification of cells per optic field positive for CD68 of the results described above. Results are shown as average + SEM. (*, $P<0.05$, Student's t-test).
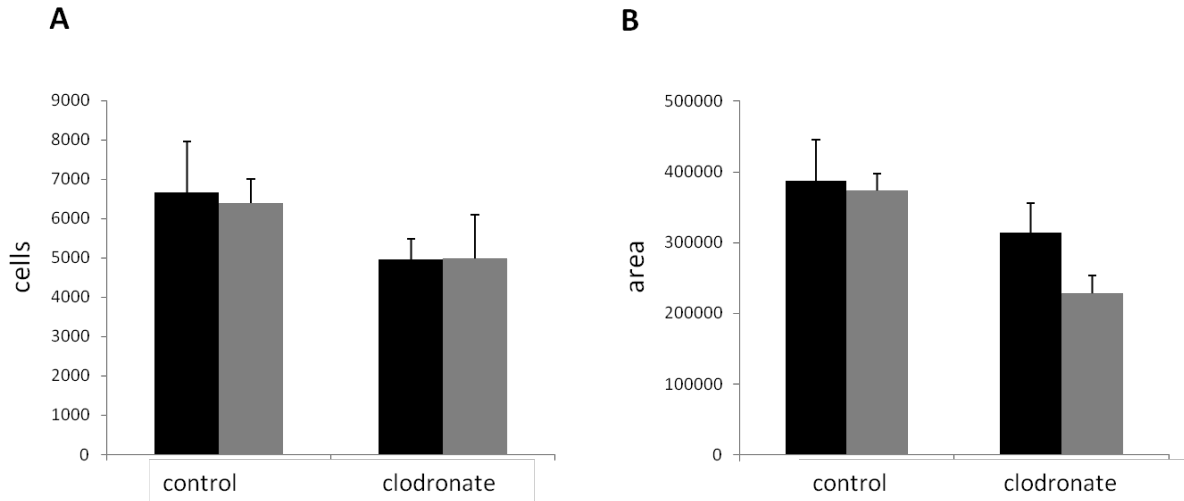
Figure S4. Effect of clodronate liposomes on involution, Related to Figure 3C. Quantification of the epithelial surface by image analysis of mammary glands from wt or Ccl8KO CB7B6 mice at involution day 2, after 5 daily ip injections of 1mg clodronate liposomes. Results are shown as average + SEM.

Transparent Methods

Animal studies

Ccl8KO mice in C57B6 background were obtained from KOMP Repository (University of California, Davis, CA, USA) and subsequently bred and maintained at the USC. SCID (C.B-17 scid) mice were obtained from Taconic (Hudson, NY, USA) and bred with Ccl8KO mice. Littermates were used for all experiments. C57B6 mice were obtained from Jackson lab and maintained at the USC. Animal studies complied with Institutional guidelines. Animal numbers for the experiments were determined based on pilot studies and depended on the number of litters for the Ccl8KO mice. The assignment to groups was performed by a different investigator from the one that acquired the measurements.

For involution studies, the number of litters of the female mice was equalized to 6 pups. For mammary gland involution initiation, females were force weaned at day 10 of lactation post-parturition. Same age nulliparous littermates were used as controls. For the qPCR

confirmation of the microarray results tissues from involution day 4 were used, similarly to the microarray study. For normal development analysis tissues from involution days 2, 5 and 7 were used to cover both the reversible and irreversible phases of involution (Lund et al., 1996, O'Brien et al., 2012).

For tumor reconstitution experiments, 2×10^5 MCF10.DCIS.com cells were resuspended in 0.2 mL of PBS and then injected subcutaneously in the mammary gland fat pad of mice (n=6), either nulliparous or at day 2 of forced weaning that followed 10 days of lactation. Animals were observed daily for tumor development. Tumor volume was calculated based on the formula (LxW2)/2. Results are shown as average + SEM (*, P<0.05 Student's t-test).

For macrophage staining during tumorigenesis, mice (n=5) were injected with 1×10^6 MCF10.DCIS.com cells resuspended in 0.2 mL of matrigel (Corning) at day 2 of forced involution that followed 10 days of lactation. Animals were sacrificed 48h later and the matrigel nodules were removed and fixed in formalin. Results are shown as average + SEM (*, P<0.05 Student's t-test). Representative images (20x) are shown.

For macrophage depletion, mice (n=5) received 5 daily intraperitoneal injections of 1mg clodronate liposomes in PBS (Liposoma B.V., Amsterdam, Netherlands) starting from lactation day 7 (van Rooijen et al., 2010). Results are shown as average + SEM.

Macrophage depletion was confirmed by immunohistochemistry for CD68 in mammary glands from wt or Ccl8KO mice (Figures S3A and S3B).

Histology

For histological analyses, mammary glands (n=3) or tumors (n=6) tumors were fixed in 10% formalin, paraffin-embedded, serially sectioned, and stained with hematoxylin/eosin. Representative images (20x or 10x) are shown.

Cell Culture

The MCF10.DCIS.com breast cancer cell line was kindly provided by Dr. Fariba Behbod (University of Kansas School of Medicine, KS) and was maintained in DMEM/F-12 supplemented with 5% Horse Serum (Corning). Cells were regularly tested for mycoplasma contamination using commercially available Mycoplasma detection kit (Myco Alert kit; Lonza).

RNA and Protein assays

Total RNA extraction from tissues was performed using RNeasy Mini Kit (Qiagen, Hilden, Germany) according to the manufacturer's protocol. cDNA was prepared with a total of 1 ug RNA using iScript™ cDNA Synthesis Kit (Bio-Rad), according to the manufacturer's protocol.

For real-time quantitative PCR, cDNA was amplified using the iTaq Universal SYBR Green Supermix (Bio-Rad) in a total reaction volume of 10 μL, using an Applied Biosystems 7300 real time instrument (Applied Biosystems) as described (Farmaki et al., 2016). *Ccl8* gene expression was assessed in the mammary glands from nulliparous mice or mice at involution day 4 (n=4,) and experiments were performed in duplicates. Results were normalized to GAPDH and are shown as average fold expression compared to nulliparous mice + SEM (*, $P<0.05$ Student's t-test).

For immunoblot analysis and Elisa CCL8 detection, mammary gland tissues from wt mice at involution day 0 (lactation day 10) (n=2), 2 (n=2), 5 (n=4), and 7 (n=4) were solubilized with ice-cold RIPA buffer (Thermo Scientific) supplemented with protease inhibitor cocktail (Thermo Scientific). CCL8 protein levels were assessed by Mouse CCL8/MCP-2 DuoSet ELISA Development kit (R&D Systems, Minneapolis, MN, USA) according to

manufacturer's protocol. Experiments were performed in duplicates and results are shown as average + SEM (*, P<0.05 Student's t-test). The protein concentration in the lysates was determined by using Bradford assay (Bio-Rad). Equal amounts of total protein were resolved by SDS–PAGE and immunoblotted for rabbit polyclonal (251309) anti-casein by Abbiotec and rabbit polyclonal anti-Gapdh 18 (5174S) by Cell Signaling. Experiments were performed thrice and representative image is shown.

Immunostaining was performed in formalin fixed, paraffin embedded sections of tissues from mice at involution day 0 (lactation day 10) (n=2-3), day 2 (n=2-3), day 5 (n=3-5), and day 7 (n=3-5) by using the Dako EnVision+ System-HRP (DAB) (K4041), following the manufacturer's instructions and counterstained with hematoxylin. The antibodies used were rat monoclonal Neutrophil Marker (NIMP-R14) sc-59338 (Santa Cruz Biotechnology) 1:50, rabbit monoclonal [SP115] anti-F/480 (ab111101), by Abcam; 1:250, mouse monoclonal Arginase I sc-271430 (Santa Cruz Biotechnology), mouse monoclonal NOS2 sc-7271 (Santa Cruz Biotechnology), mouse monoclonal CD68 sc-20060 (Santa Cruz Biotechnology). Negative controls included non-immune serum instead of antibody. The number of stained cells (5 random optic fields per sample) as well as the number of total cells were quantified using ImageJ software (National Institutes of Health, USA). Evaluation of samples was performed blindly. Images shown were obtained by a Leica ICC50 HD (Buffalo Grove, IL, USA). Results are shown as average + SEM (*, P<0.05, **, P<0.001 Student's t-test) and representative images (40x) are shown.

Quantification and Statistical Analysis

Quantification of the bands and pictures was performed by ImageJ. All data are presented as average values of samples, error bars correspond to standard error of the mean (SEM) unless

otherwise stated. Statistical analysis of the results was performed using Student's two tailed *t* test. The results were considered statistically significant when P-value <0.05.

Oligonucleotides

Mouse Ccl8 primers	Mouse GAPDH primers
5′-TTCCAGCTTTGGCTGTCTCT-3′ 5′-GGGTGCTGAAAAGCTACGAG-3′	5′-ACCCAGAAGACTGTGGATGG-3′ 5′-CACATTGGGGGTAGGAACAC-3′

Supplemental References

Farmaki, E., Chatzistamou, I., Kaza, V. and Kiaris, H. (2016). A CCL8 gradient drives breast cancer cell dissemination. *Oncogene* **35**, 6309-6318.

Lund, L. R., Romer, J., Thomasset, N., Solberg, H., Pyke, C., Bissell, M. J., Dano, K. and Werb, Z. (1996). Two distinct phases of apoptosis in mammary gland involution: proteinase-independent and -dependent pathways. *Development* **122**, 181-193.

O'Brien, J., Martinson, H., Durand-Rougely, C. and Schedin, P. (2012). Macrophages are crucial for epithelial cell death and adipocyte repopulation during mammary gland involution. *Development* **139**, 269-275.

van Rooijen, N. and Hendrikx, E. (2010). Liposomes for specific depletion of macrophages from organs and tissues. *Methods Mol. Biol.* **605**, 189-203.